Needle Steering Modeling and Analysis using Unconstrained Modal Analysis

Kaiguo Yan[1], Wan Sing Ng[1] Keck Voon Ling[2]
[1]CIMI Lab, MAE,
[2]EEE,
Nanyang Technological University,
Singapore,
yank0001@ntu.edu.sg

Yan Yu[3], Tarun Podder[3]
[3]Dept. of Radiation Oncology, University of Rochester Medical Center, New York, U.S.A

Tien-I Liu[4]
[4]Computer Integrated Manufacturing Lab, California State University, Sacramento, California, U.S.A

CWS Cheng[5]
[5]Dept. of Urology Singapore General Hospital, Singapore

Abstract **– Precise needle placement is very important for a number of percutaneous interventions. Poor placement may cause tissue damage, misdiagnosis, poor dosimetry and tumor seeding. Yet precise needle placement is hard to achieve in real practice due to tissue heterogeneity and elastic stiffness, unfavorable anatomic structures, needle bending, inadequate sensing, tissue/organ deformation and movement, and poor maneuverability. To date, there are few effective physical-based needle steering systems exist that can correct the needle deflection in real time. In addition, many procedures are currently not amenable to needles because of obstacles, such as bone or sensitive tissues, which lie between feasible entry points and potential targets. Thus, there is a clear motivation for needle steering in order to provide accurate and dexterous targeting.**

In this paper, a spring-beam-damper system is proposed to model the system dynamics while applying steering force on the needle end. Instead of using the traditional finite element method, unconstrained model analysis is adopted to derive the system dynamic equations. The modeling procedure and analysis method are given in details. Experiment had also been carried out to verify the accuracy of the proposed model. Conclusions and future works are given in subsequent sections.

Index Terms- **Needle steering modeling, unconstrained modal analysis**

I. BACKGROUND

Needle insertion is a critical aspect of many medical diagnoses, treatments and scientific studies, including percutaneous procedures requiring therapy delivery to, or sample removal from, a specific location, which may be deeply seated inside the human body. Percutaneous procedures involving such flexible instrument insertions include vaccinations, blood/fluid sampling, regional anesthesia, tissue biopsy, catheter insertion, cryogenic ablation, electrolytic ablation, brachytherapy, neurosurgery, deep brain stimulation etc. Precise needle placement is very important. Poor placement may cause tissue damage, misdiagnosis, poor dosimetry and tumor seeding. Yet precise needle placement is hard to achieve in real practice due to tissue heterogeneity and elastic stiffness, unfavorable anatomic structures, needle bending, inadequate sensing, tissue/organ deformation and movement, and poor maneuverability. Several research groups (e.g. [1,2]) have implemented computer and robotic assistance to align the needle with the target assuming known target location in 3D, target immobilization, and a straight needle path. Errors caused by needle deflection and tissue deformation have been observed for a long time. Yet to date, there are few effective physical-based needle steering systems exist for correcting the needle deflection. In addition, many procedures are currently not amenable to needles because of obstacles, such as bone or sensitive tissues, which lie between feasible entry points and potential targets. Thus, there is a clear motivation for needle steering in order to provide accurate and dexterous targeting.

Flexible needle steering was first addressed by DiMaio *et al*. [3]. He used a large-strain elastic needle model coupled with the two-dimensional tissue models to simulate needle and tissue phantom motion, as well as to predict target motion and needle trajectories due to phantom and needle deformations. The traditional finite element model was used to solve the system kinematics. The computation involves solving the two-dimensional finite element mesh of the tissue and iterative nonlinear flexion of a beam, and requires nine independent computations for devising the Jacobian elements. So the computation complexity involved in does not allow real-time simulation and control of the system.

Recently, a research group [4] proposed a method to estimate needle and soft tissue interaction for the simulation of accurate seed placement in prostate brachytherapy. They imbedded stainless steel beads into the soft tissue and used 2 C-ARM Fluoroscopes, which were placed orthogonal to each other, to obtain in real time 3D needle trajectory and internal global and local tissue deformation during needle insertion. The obtained data were used to extract the parameters for final used in FEM

simulation. Compared with DiMaio's method, this method seems more realistic to the real tissue. They adopted FEM to calculate the local Effective Modulus iteratively. While at the same time, it becomes more computation expensive.

Some researchers from Johns Hopkins University [5,6] proposed a nonholonomic model for steering flexible bevel-tip needles in rigid tissues. The nonholonomic model, a generalization of a 3 degree-of freedom bicycle model, was experimentally validated using a very stiff tissue phantom. Reachability is a critical issue involved in this approach.

In a recent MICCAI conference, Daniel Glozman and Moshe Shoham [7] presented a simplified virtual spring model that allowed fast path planning and real time tracking for the needle insertion procedure. They assumed small tissue displacement and linear lateral force response. So the tissue forces on the needle could be modeled as lateral virtual springs distributed along the needle curve plus friction forces tangent to the needle longitudinal axis. Modeling of a flexible needle was based on the assumption of quasistatic motion, so the needle is in equilibrium state at each step. They adopted the nodal degrees of freedom from finite elements theory, in which the coordinates were specifically identified with a single nodal point and represented a displacement or rotation. A third degree polynomial was used to calculate the displacement of each element. Compromise had to be made between the computation efficiency and the model accuracy. In this paper, the accuracy of the model was not reported.

In this paper, a spring-beam-damper system is proposed with the consideration of both the linear and nonlinear tissue reaction effects when interacting with the flexible needle. In the literature, the spring-damper model has been adopted by many research groups [8,9,10] in studying the tissue deformation. However, how the instrument interacts with soft tissue and how to control the instrument while in collision with such environment have received little attention. Some researchers e.g.[11,12] studied the collision of the flexible link with the environment in the application of grinding or surface turning operation. They modeled the environment as a simple spring-damper system, which was assumed to be stationary and was arbitrarily placed along the trajectory such that the beam would only make contact with it at the tip. In the application of needle insertion, the flexible instrument interacts with the environment with changing force along the needle body from time to time. The situation is much more complicated compared with the point contact. The traditional way to solve such kind of problem is to use finite element method, which is computationally inefficient. In this work, we adopt unconstrained modal analysis method to solve the dynamics of the spring-beam-damper system. The detailed modeling procedure and analysis method are given in this paper. Experiment has also been carried out to test accuracy of the proposed model and the results are reported in this paper. Conclusions and future works are given in subsequent sections.

II. Needle Steering Modeling and Analysis

A. Model description

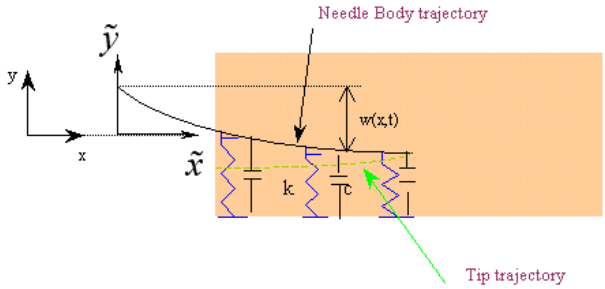

Fig. 1 Mechanism of the needle insertion procedure

The spring-beam-damper system is considered in this study. Fig. 1 shows the mechanism of the needle insertion procedure. The flexible needle is assumed to follow the Bernoulli-Euler beam model and to be clamped tightly at end. The tissue is represented by a series of spring-damper system. The initial lengths of springs are decided by the needle tip trajectory. At the beginning, the needle is placed next to the tissue. With time progressing on, the needle inserts into the tissue. Then the springs and dampers come into contact with the needles inside the body and exert force on it accordingly. The forces of the springs at time instant t are determined by the needle body shape at that time and the forces of the dampers are determined by the velocities of the contact points.

To derive the equations of needle insertion, the following assumptions are made:

(1) For simplicity, the needle is considered to move only in the XY plane. X is the insertion direction and Y is the steering direction.
(2) There is no longitudinal compression of the beam and only lateral deflection is possible. Furthermore, the lateral deflection of the beam is small compared with the length of the beam.
(3) The rotational effect of the beam with respect to the local co-ordinate system is neglected.
(4) At current stage, we assume the springs and dampers in the system have constant coefficients. Later we will generalize them into time-varying or distance-varying based on scientific studies or observations.

Under the above assumptions, the system dynamic equation can be derived using Hamilton's principle as follows:

$$\int_{t_1}^{t_2} (\delta T - \delta V + \delta W_{nc}) dt = 0 \qquad (1)$$

T: kinetic energy
V: potential energy
W_{nc} : work done by non-conservative forces

A local coordinate system is introduced by the Galilean transformation to replace the fixed coordinates (x) with a moving coordinate system ($\tilde{x}$), which is attached at the need end and moves with it. v_x is the needle insertion velocity.

$$\tilde{x} = x - v_x t \quad \text{and} \quad \tilde{y} = y$$

The Galilean transformation fulfills the following relationships.

$$\frac{\partial}{\partial x} = \frac{\partial}{\partial \tilde{x}}; \left.\frac{\partial}{\partial t}\right|_x = \left.\frac{\partial}{\partial t}\right|_{\tilde{x}} - v_x \frac{\partial}{\partial \tilde{x}},$$

$$\left.\frac{\partial^2}{\partial t^2}\right|_x = \left.\frac{\partial^2}{\partial t^2}\right|_{\tilde{x}} - \partial v_x \left.\frac{\partial^2}{\partial \tilde{x} \partial t}\right|_{\tilde{x}} + {v_x}^2 \frac{\partial^2}{\partial \tilde{x}^2}$$

The system kinetic energy T and potential energy V are given as follows.

$$T = \frac{1}{2} M \dot{y}^2 + \int_0^l \frac{1}{2} \rho (\dot{y}(t) + \dot{\omega}(\tilde{x}, t))^2 d\tilde{x} = T(\dot{y}, \dot{\omega}) \tag{2}$$

$$\begin{aligned} V = & \int_0^l \frac{1}{2} EI \omega''^2 d\tilde{x} + \int_0^l H(\tilde{x} - l + v_x t) \cdot \frac{1}{2} k_0 [y(t) + \omega(\tilde{x}, t) \\ & - y(t + \frac{\tilde{x} - l}{v_x}) - \omega(L, \frac{\tilde{x} - l}{v_x} + t)]^2 d\tilde{x} \xleftarrow{h(t) = l - v_x t} \\ & \int_0^l \frac{1}{2} EI \omega''^2 d\tilde{x} + \int_0^l H(\tilde{x} - h(t)) \cdot \frac{1}{2} k_0 [y(t) + \omega(\tilde{x}, t) \\ & - y(\frac{\tilde{x} - h(t)}{v_x}) - \omega(L, \frac{\tilde{x} - h(t)}{v_x})]^2 d\tilde{x} \end{aligned} \tag{3}$$

where M is the mass of the fixture, which links the needle with the 3D motion platform. L is the length of the elastic beam, ρ is the mass per unit length of the elastic beam, E is the Young's modular, I is the second moment of area about the z axis. k_0 is stiffness coefficient of the spring per unit length, and c is that of the damper. $\dot{\omega} = \partial \omega(x,t) / \partial t$ and $\omega'' = \partial^2 \omega(x,t) / \partial x^2$ where w(x, t) is the deflection of the beam at x at time t.

H is the Heaviside unit step function.

$$H(x) = \begin{cases} 1 \ldots x \geq 0 \\ 0 \ldots x < 0 \end{cases}$$

The virtual work done by all the non-conservative forces (steering force F_y and damping forces), is given by

$$\delta W_{nc} = F_y \cdot \delta y - \int_0^l H(\tilde{x} - l + v_x t) \cdot c(\dot{y} + \dot{w}) \cdot \delta(y + w) d\tilde{x} \tag{4}$$

The equation of motion and the boundary conditions of the system are obtained by substituting the above equations (2)-(4) into (1), integrating the resulting equation by parts and considering that the time t1 and t2 are arbitrary and that $\delta x, \delta w, \delta h$ are arbitrary and independent. The equations of motion for the spring-damper system are obtained as follows:

$$\begin{aligned} F(y,t) = & M\ddot{y} + \int_0^L \rho(\ddot{y} + \ddot{\omega}) d\tilde{x} + \int_0^L H(\tilde{x} - L + v_x t)[k_0(y + \omega(\tilde{x}, t) \\ & - y(t_1) - \omega(L, t_1)) + c(\dot{y} + \dot{\omega}(\tilde{x}, t))] d\tilde{x} \end{aligned} \tag{5}$$

$$\begin{aligned} & EI\omega'''' + \rho(\ddot{y} + \ddot{\omega}) + H(\tilde{x} - L + v_x t)[k_0(y + \omega(\tilde{x}, t) \\ & - y(t_1) - \omega(L, t_1)) + c(\dot{y} + \dot{\omega}(\tilde{x}, t))] = 0 \end{aligned} \tag{6}$$

$$t_1 = t + \frac{\tilde{x} - L}{v_x}$$

Boundary conditions:

(1) $w(x,0) = w(0,t) = 0$ (2) $w'(0,t) = 0$

(3) $w''(L,t) = w'''(L,t) = 0$

B. Model analysis

To solve the partial differential equations shown in (5) and (6), unconstrained modal analysis was adopted in this approach. By unconstrained modal analysis [13], the deflection of the beam at $\tilde{x}$, ω($\tilde{x}$,t) and the position of the fixture, y(t) can be represented, respectively, as

$$y = \alpha(t) + \beta q(t) \tag{7}$$

$$\omega(\tilde{x}, t) = \phi(\tilde{x}) q(t) \tag{8}$$

where α(t) describes the motion of the center of mass of the total system without perturbation. This allows transforming the nonhomogeneous equations into a set of second-order ordinary differential equations.

Substitute equations (7) into (5), we get

$$M_t \ddot{\alpha}(t) = F_y(t) - f(t)$$

$$f(t) = \int_0^L H(\tilde{x} - L + v_x t)[k_0(y + \omega(\tilde{x}, t) - y(t_1) - \omega(L, t_1)) + c(\dot{y} + \dot{\omega}(\tilde{x}, t))] d\tilde{x}$$

$$M_t = M + \rho L$$

if β satisfies

$$\beta_j = -\frac{\rho}{M_t} \int_0^L \phi_j(\tilde{x}) d\tilde{x} = -\frac{\rho}{M} \int_0^L \varphi_j(\tilde{x}) d\tilde{x} \tag{9}$$

and

$$\varphi(\tilde{x}) \triangleq \beta + \phi(\tilde{x})$$

To get the normal mode solutions, where the effect of the external force vanishes, one can decompose (6) into two equations as follows

$$\ddot{q}(t)+\omega^2 q(t)=0 \tag{10}$$

$$EI\varphi''''(\tilde{x})-\omega^2\rho\varphi(\tilde{x})=0 \tag{11}$$

where ω is the natural frequency of the system, and the boundary conditions become

$$\varphi(0)=\beta,\ \varphi'(0)=0,\ \varphi''(L)=0,\ \varphi'''(L)=0 \tag{12}$$

Assumed-mode solutions for a finite number of eigenvalues are obtained form previous development by considering the first n terms. The deflection of the elastic beam and the displacement of the fixture are expressed, respectively, in terms of n mode shapes using the obtained $\varphi(\tilde{x}), \beta_i, q_i(t)$ as follows

$$w(\tilde{x},t)=\sum_{i=1}^{n}\phi_i(\tilde{x})q_i(t)=\sum_{i=1}^{n}[\varphi_i(\tilde{x})-\beta_i]q_i(t) \tag{13}$$

and accordingly, the position of fixture is given as

$$y(t)=\alpha(t)+\sum_{i=1}^{n}\beta_i q_i(t) \tag{14}$$

Substituting (9),(10),(11) into (6), multiplying both sides of the resulted equation by $\phi_i(\tilde{x})$, integrating over the problem domain and applying the orthogonal condition, one obtains:

$$\begin{aligned}&\dot{\alpha}(t)\int_{L-v_x t}^{L}c\varphi_i(\tilde{x})d\tilde{x}+\alpha(t)\int_{L-v_x t}^{L}k_0\varphi_i(\tilde{x})d\tilde{x}\\&+\ddot{q}_i(t)+\sum_j\dot{q}_j(t)\int_{L-v_x t}^{L}c\varphi_i(\tilde{x})\varphi_j(\tilde{x})d\tilde{x}\\&+\sum_j q_j(t)\int_{L-v_x t}^{L}k_0\varphi_i(\tilde{x})\varphi_j(\tilde{x})d\tilde{x}+\omega_i^2 q_i(t)\\&=F_y\beta_i+f_{1i}\end{aligned} \tag{15}$$

$$\begin{aligned}&M_t\ddot{\alpha}(t)+cv_x\dot{\alpha}(t)t+\sum_j\dot{q}_j(t)\int_{L-v_x t}^{L}c\varphi_j(\tilde{x})d\tilde{x}\\&+\sum_j q_j(t)\int_{L-v_x t}^{L}k_0\varphi_j(\tilde{x})d\tilde{x}+k_0v_x\alpha(t)t\\&=F_y+f_2\end{aligned} \tag{16}$$

$$\begin{aligned}f_{1i}&=\int_0^t k_0\alpha(t_1)\varphi_i(v_x t_1+L-v_x t)v_x dt_1\\&\quad+\int_0^t k_0\sum_j\varphi_j(L)q_j(t_1)\varphi_i(v_x t_1+L-v_x t)v_x dt_1\\&=\int_0^t k_0 Y(t_1)\varphi_i(v_x t_1+L-v_x t)v_x dt_1\end{aligned} \tag{17}$$

$$\begin{aligned}f_2&=\int_0^t k_0\alpha(t_1)v_x dt_1+\int_0^t k_0\sum_j\varphi_j(L)q_j(t_1)v_x dt_1\\&=\int_0^t k_0 Y(t_1)v_x dt_1\end{aligned} \tag{18}$$

III. Preliminary Experimental Verification

To validate the effectiveness of the proposed model, quantitative experiment has been carried out. The flowchart of verification method is shown in Fig. 2. The needle is driven by the 3DOF platform into the phantom. The needle tip position and corresponding needle end force data are collected during the procedure. The collected force data are then filled into the simulation model as the input. At last, the simulated output, tip position data are compared with the real deflection measured during experiments.

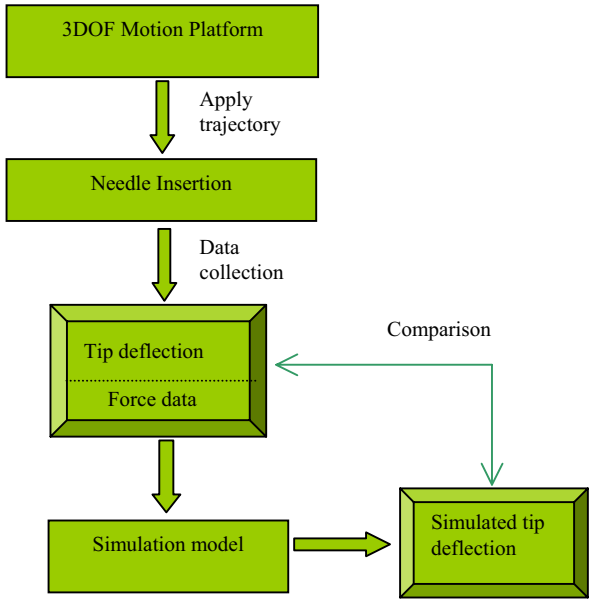

Fig. 2: Flowchart of the verification method

The experimental setup shown in Fig.3 is used to carry out the experiment. A rectangular slab of elastic material made of gelatin is used at current stage to represent the human tissue. The 3 Degree-of-Freedom (DOF) motion platform drives the needle into the phantom following some designed trajectory. A 6 DOF force/torque (F/T) sensor (Nano17-SI-12-0.12 ® from ATI Industrial Automation, USA) is mounted at the needle end of the needle to measure the needle end force. The needle adopted here is a 5-DOF MagTrax Needle Probe (from Traxtal Technology, Canada). It is a 130mm long needle and has a sensor located at the stylet's proximal tip. This needle movement can be observed in real time via an electromagnetic system called Aurora® (from Northern Digital Inc. Canada). It has a Field Generator that can generate a known electromagnetic field with a characterized measurement volume of 500mm*500mm*500mm. When the tools with the sensor

coils are exposed to this field, their position can be calculated regardless of the tool's bending and does not subject to the line-of-sight limitations that affect the optical tracking systems. During the insertion, the needle tip position can be tracked regardless of deformation or deflection.

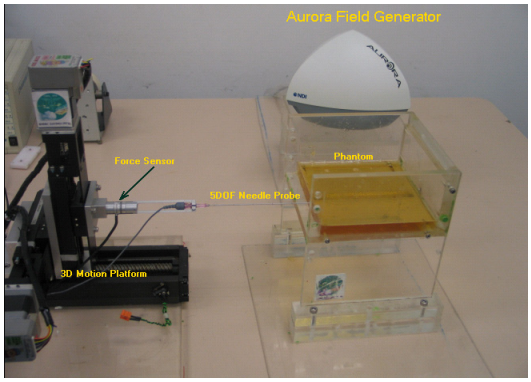

Fig. 3 Experiment setup

The needle was driven into the phantom with insertion speed at 5mm/s and steering speed at 1.25mm/s. The needle tip trajectory was collected and compared with the simulation result. At the beginning, the reaction force from the phantom was low. So the needle tip moved in the same direction as the steering force. With the reaction force from the phantom increased, the needle tip began to move to the opposite direction. The tracked needle tip vs. simulated needle tip were compared and shown in Fig. 4. The big drop-down at the beginning was caused by the sensor noise. We can see that the proposed model has predicted the needle tip trajectory quite well. More experiments will be carried out in the near future to further validate this model.

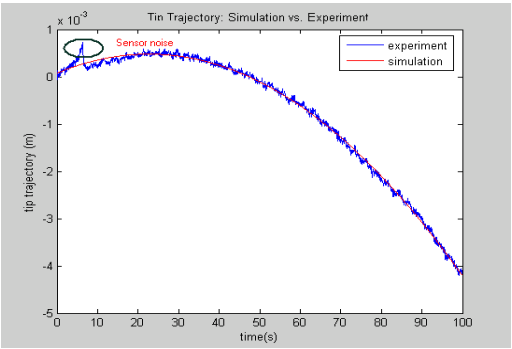

Fig. 4 Experiment vs. Simulation

IV. Conclusions and Future works

In this work, we focus on the modeling of the dynamics of steering force and movement in y direction, which is normal to the insertion direction x. In the literature, the needle insertion force has been studied by many research groups in gelatin [14], *ex vivo* porcine, human and bovine samples [15,16]. The influences of the needle coating [17], needle dimension, tip shape and insertion velocity [18] etc. to the insertion force have also been explored exhaustively. Mostly recently, some researchers [19] published their work on the needle insertion force modeling, which separated the cutting, stiffness and friction force and modeled them separately. Our objective here is to correct the needle deflection or steer the needle trajectory to avoid the obstacles during penetration. The steering force-movement, other than the insertion force-movement, will be our main focus. In future, we will also build the insertion model from experimental data and supplement it into our final control model to keep the needle insertion at constant velocity while doing the adjustment.

Presently, we are only using phantoms, which are easier to control. Properties like the spring and damper coefficients can be decided in advance. But later when applying to human, it's hard to decide these coefficients beforehand. So in the near future, we will also design an online parameter estimator, which can estimate the parameters in real time. Our final objective is to use the proposed model to design an adaptive needle steering system that can steer the needle tip to reach a designated position precisely.

ACKNOWLEDGEMENT

The authors would like to thank the colleagues in CIMI Lab and the final year project student Seetha for their assistance in carrying out the experiment. Nanyang Technological University (Singapore), NMRC 0859/2004, US National Cancer Institute (NCI) (under grant R01 CA091763) are also acknowledged for support.

REFERENCE

[1] Loser, M, Navab, N (2000), "A new robotic system for visually controlled percutaneous interventions under CT", Proceedings to Medical Image Computing and Computer-Assisted Intervention, 2000; Lecture notes in computer science, Vol 1935, Springer Verlag, 2000, pp. 887-897.

[2] Stoianovici, D., Cadeddu, J. A., Demaree, R. D., Basile, H. A., Taylor, R. H., Whitcomb, L. L., Sharpe, W. N. Jr., Kavoussi, L. R, "An Efficient Needle Injection Technique and Radiological Guidance Method for Percutaneous Procedures", Lecture Notes in Computer Science, 1997 CVRMed-MRCAS, Springer-Verlag, Vol. 1205, pp.295-298.

[3] Simon P. DiMaio, Modelling, "Simulation and Planning of Needle Motion in Soft Tissues", PhD thesis, September 2003, The University of British Columbia.

[4] James Hing, Ari D. Brooks, and Jaydev P. Desai, "Reality-based Estimation of Needle and Soft-tissue Interaction for Accurate Haptic Feedback in Prostate Brachytherapy Simulation", International Symposium of Robotics Research, San Francisco, October 12-15, 2005.

[5] Wooram Park, Jin Seob Kim, Yu Zhou,etc. "Diffusion-Based Motion Planning for a Nonholonomic Flexible Needle Model", in Proc. IEEE Int. Conf. on Robotics and. Automation, Apr. 2005, pp.4611–4616.

[6] R. Webster, N. Cowan, G. Chirikjian, and A. Okamura, "Nonholonomic Modeling of Needle Steering," 9th International Symposium on Experimental Robotics, Singapore, 2004.

[7] Daniel Glozman, Moshe Shoham, "Flexible Needle Steering and optimal Trajectory Planning for Percutaneous Therapies", MICCAI 2004

[8] D. Terzopoulos and K. Waters (1993). "Analysis and synthesis of facial image sequences using physical and anatomical models". IEEE Transactions on Pattern Analysis and Machine Intelligence, vol. 15, pp. 569-579

[9] F. Boux de Casson and C. Laugier (1999). "Modelling the dynamics of a human liver for a minimally invasive surgery simulator".

MICCAI, vol. 1679 of Lecture Notes in Computer Science, pp. 1156-1165
[10] P. F. Neumann, L. L. Sadler, and J. G. M.D. (1998). “Virtual reality vitrectomy simulator”. MICCAI, pp. 910-917
[11] Ming-Chyuan Lu,Elijah Kannatey-Asibu,Jr., Flank Wear and Process Characteristic Effect on System Dynamics in Turning, Journal of Manufacturing Science and Engineering,2004
[12] Francis M.C.Ching and Dvid Wang, Exact Solution and Infinite-Dimensional Stability Analysis of a Single Flexible Link in Collision,IEEE Transactions on Robotics and Automation,VOL>19,No.6,December 2003
[13] Carlos Canudas de Wit etc., Theory of Robot Control, Springer
[14] L. Hiemenz, A. Litsky, and P. Schmalbrock (1997). “Puncture Mechanics for the Insertion of an Epidural Needle”. 21st Annual Meeting of the American Society of Biomechanics, Available Online: http://asb-biomech.org/onlineabs/abstracts97/34/index.html
[15] P. N. Brett, T. J. Parker, A. J. Harrison, T. A. Thomas, and A. Carr (1997). “Simulation of resistance forces acting on surgical needles”. Inst. of Mech. Eng. Part H, Journal of Engineering in Medicine, vol. 211, pp. 335–347
[16] C. Simone and A. M. Okamura (2002). “Haptic Modeling of Needle Insertion for Robot-Assisted Percutaneous Therapy”. Proceedings of the IEEE International Conference on Robotics and Automation, pp. 2085-2091
[17] T.K. Podder, J. Sherman, D.P. Clark, D. Fuller, D.J. Rubens, E.M. Messing, J.G. Strang, L. Liao, W.S. Ng, and Y. Yu, “Evaluation of the Effects of Coating on Surgical Needle Intervention,” in the Proceedings of the 3rd European Medical & Biological Engineering Conference (EMBEC), Prague, Czech Republic, November 20-25, 2005.
[18] T.K. Podder, D.P. Clark, D. Fuller, J. Sherman, W.S. Ng, etc, “ Effects of Velocity Modulation during Surgical Needle Insertion”, IEEE EMBS-2005,Shanghai
[19] Allison M. Okamura, Christina Simone, and Mark D. O’Leary, “ Force Modeling for Needle Insertion into Soft Tissue”, IEEE Transactions on Biomedical Engineering, No 10, Vol.51, Oct. 2004

TABLE I
LIST OF SYMBOLS

M	The mass of the fixture
Mt	Total mass of the needle and fixture
vx	Needle insertion velocity
E	Young’s modular
I	The second moment of area about the z axis
L	The length of the elastic beam
ρ	The mass per unit length of the elastic beam
k0	Stiffness coefficient of the spring
c	Stiffness coefficient of the damper
w(x, t)	The deflection of the beam at x at time t.
ω	The natural frequency of the system
y(t)	The position of fixture
Fy	Steering force applying on the needle end